

~~195  
3-1-85~~

9MC

3

DOE/FE/60177-1664  
(DE85001459)

DR-0831-1

## INVESTIGATION OF TRACER TESTS ON THE WESTERN RESEARCH INSTITUTE'S 10-TON RETORT

By  
T. Fred Turner  
Dennis F. Moore

May 1984

Work Performed Under Contract No. FC21-83FE60177

For  
U. S. Department of Energy  
Morgantown Energy Technology Center  
Laramie, Wyoming

By  
Western Research Institute  
Laramie, Wyoming

MASTER

Technical Information Center  
Office of Scientific and Technical Information  
United States Department of Energy



## **DISCLAIMER**

**This report was prepared as an account of work sponsored by an agency of the United States Government. Neither the United States Government nor any agency Thereof, nor any of their employees, makes any warranty, express or implied, or assumes any legal liability or responsibility for the accuracy, completeness, or usefulness of any information, apparatus, product, or process disclosed, or represents that its use would not infringe privately owned rights. Reference herein to any specific commercial product, process, or service by trade name, trademark, manufacturer, or otherwise does not necessarily constitute or imply its endorsement, recommendation, or favoring by the United States Government or any agency thereof. The views and opinions of authors expressed herein do not necessarily state or reflect those of the United States Government or any agency thereof.**

## **DISCLAIMER**

**Portions of this document may be illegible in electronic image products. Images are produced from the best available original document.**

## DISCLAIMER

This report was prepared as an account of work sponsored by an agency of the United States Government. Neither the United States Government nor any agency thereof, nor any of their employees, makes any warranty, express or implied, or assumes any legal liability or responsibility for the accuracy, completeness, or usefulness of any information, apparatus, product, or process disclosed, or represents that its use would not infringe privately owned rights. Reference herein to any specific commercial product, process, or service by trade name, trademark, manufacturer, or otherwise does not necessarily constitute or imply its endorsement, recommendation, or favoring by the United States Government or any agency thereof. The views and opinions of authors expressed herein do not necessarily state or reflect those of the United States Government or any agency thereof.

This report has been reproduced directly from the best available copy.

Available from the National Technical Information Service, U. S. Department of Commerce, Springfield, Virginia 22161.

Price: Printed Copy A03  
Microfiche A01

Codes are used for pricing all publications. The code is determined by the number of pages in the publication. Information pertaining to the pricing codes can be found in the current issues of the following publications, which are generally available in most libraries: *Energy Research Abstracts (ERA)*; *Government Reports Announcements and Index (GRA and I)*; *Scientific and Technical Abstract Reports (STAR)*; and publication NTIS-PR-360 available from NTIS at the above address.

DOE/FE/60177-1664  
(DE85001459)  
Distribution Category UC-91

INVESTIGATION OF TRACER TESTS ON THE  
WESTERN RESEARCH INSTITUTE'S 10-TON RETORT

By  
T. Fred Turner  
Dennis F. Moore

May 1984

Work Performed Under Cooperative Agreement  
DE-FC21-83FE60177

For  
U. S. Department of Energy  
Office of Fossil Energy  
Morgantown Energy Technology Center  
Laramie Project Office  
Laramie, Wyoming

By  
Western Research Institute  
Laramie, Wyoming

## SUMMARY

An oil shale rubble bed with contrasting permeability regions is investigated using a gas tracer in conjunction with a two-dimensional flow and tracer model and with a one-dimensional dispersion model. Six runs on the retort are discussed. Tracer injections are made into the main flow inlet and into five taps near the top of the retort. Detection taps are located at four levels in the retort with five taps on each level. The one-dimensional dispersion model is fit to the tracer response curves producing estimates of dispersion and space:time in the retort. The dispersion model produces reasonable estimates where the fluid flow deviates only slightly from vertical. The two-dimensional flow model developed by Travis at Los Alamos National Laboratory (LANL) is compared to tracer velocities. The correlation between the model and the data is good in the last of the six tests. The correlation is not as good in the earlier tests, and possible reasons for this are discussed.

## INTRODUCTION

The Western Research Institute (WRI) at Laramie, Wyoming, is conducting tracer and retorting tests on oil shale rubble beds with regions of flow blockage and flow channeling. These types of rubble bed non-uniformities are common in large modified in situ (MIS) oil shale retorts and are important because severe flow blockage or channeling causes reduced oil yields. The 150-ton retort is being used for the flow blockage experiment reported elsewhere<sup>[1]</sup> and the 10-ton retort is being used for the flow channeling tests. Progress on the tracer and flow modeling work on the 10-ton retort tests is described in this report. Retorting procedures and results are discussed elsewhere.<sup>[2]</sup> This work is done under Cooperative Agreement DE-FC21-83FE60177 with the U.S. Department of Energy.

A pre-retorting diagnostic technique such as tracer testing is needed to evaluate rubble nonuniformities. If an oil shale rubble bed is not uniform, or in other words has a spatially varying void fraction or particle size, then oil yield may be reduced. It is important that the nonuniformities be understood so that retorting procedures can be optimized. The 10-ton retort tests have been designed to evaluate the effects of both flow channel size and particle size on retorting efficiency and to study the effectiveness of tracer testing for determining rubble bed and flow parameters.

To date, six of nine planned retorting tests have been completed. The results of the tracer tests on these six runs are to be discussed in this report. Also included is a comparison of the tracer results with a two dimensional flow and tracer model.

## EXPERIMENT

### Retort Configuration

The 10-ton oil shale retort located north of Laramie, Wyoming, is the vessel chosen for the flow channeling portion of WRI's nonuniform rubble bed tracer studies. This retort is small enough to allow a relatively short turn-around time on retorting tests and yet is large enough to allow loading with nearly full-scale particle sizes. As shown in Figure 1, the 10-ton retort is a 1.8 meter (6 foot) diameter by 3.7 meter (12 foot) high refractory lined steel shell. The bottom of the retort has a steel grate to support the shale and both the top and the bottom have hinged semispherical covers. The retort is lined with a 0.114 meter (4.5 inches) thick layer of fire brick and a 0.114 meter (4.5 inches) thick layer of castable insulating material and an insulating fiber blanket, causing the inside diameter to be 1.37 meters (4.5 feet).

The test program for the flow channeling experiments on the 10-ton retort calls for the retort to be loaded in a fashion that creates a permeability contrast between a core region and a surrounding annulus. The effects of varying the core channel size and the particle size in that channel are being studied. A schematic of the retort with the contrasting permeability core is shown in Figure 1. The top of the core is approximately 0.6 meters (24 inches) below the flange at the retort top and the bottom of the core rests on a protective rock base. The diameter of the core is 0.30, 0.46, or 0.61 meters (12, 18 or 24 inches) depending on the test. The test schedule, as described in Table 1, is for the first six of nine planned tests. For tests S71 through S74 the region above the core is filled with the same size shale as the annulus. In tests S75 and S76 the shale in the top region is different for

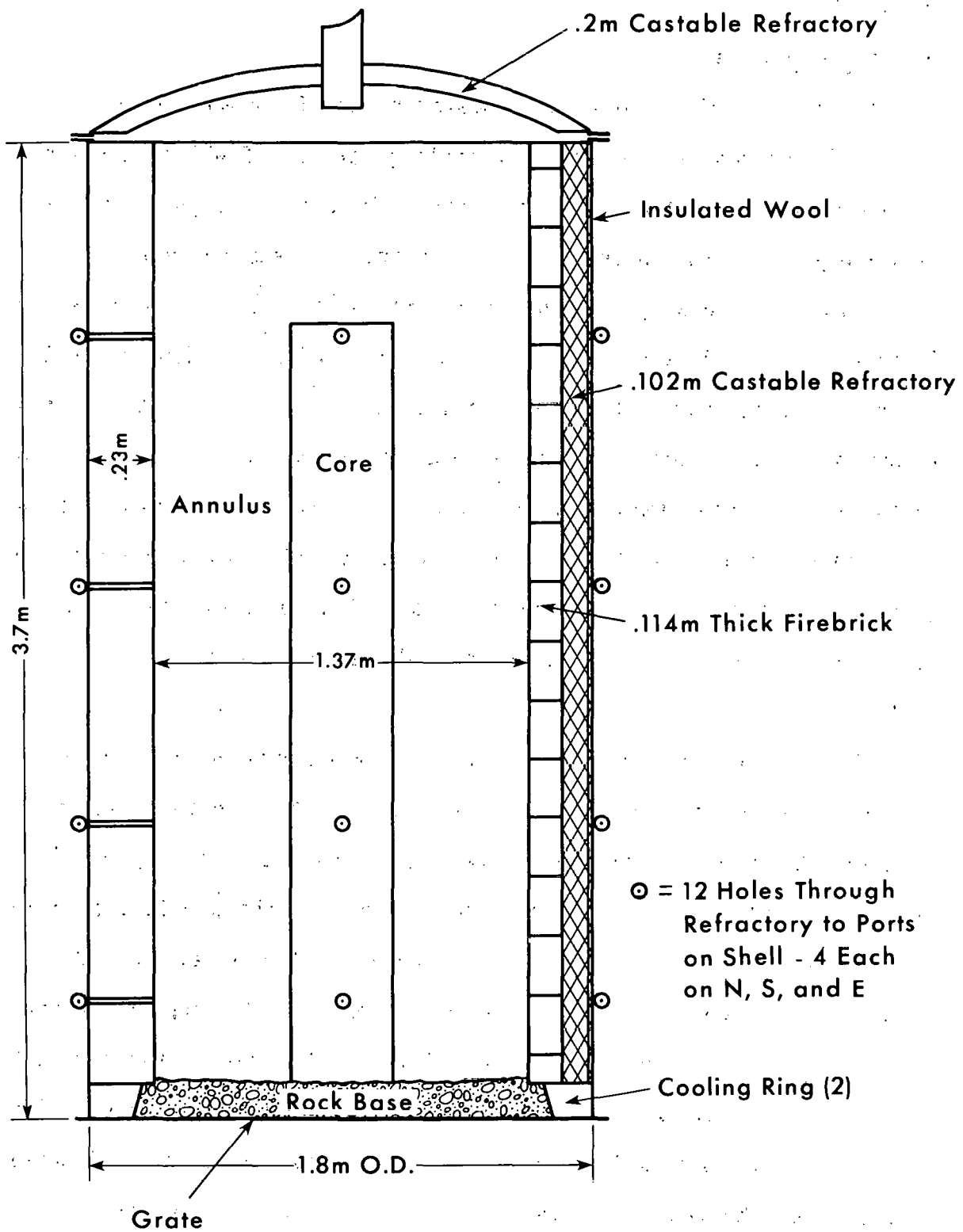


Figure 1. Ten Ton Retort

reasons that are discussed later.

### Retort Loading

The retort is loaded using a bucket and an overhead crane. A layer of granite is spread over the grate to prevent the grate from overheating and then the shale is loaded. To produce the core region of the retort three short cylinders have been constructed having the diameters required for the different tests. For a given test the appropriate cylinder is placed on the rock base at the center of the retort; the cylinder is filled and then is covered while shale is dumped into the annulus. The cylinder is pulled upwards until the bottom is at the surface of the shale. It is then reloaded and the procedure is repeated. Each cylinder is slotted to allow placement of tracer probes and thermocouples.

Shale in five size ranges is used for the flow channeling tests. The screen analyses of the shale are shown in Table 2 with the corresponding weighted average sizes. The average size is calculated from equation 1.

$$\text{where } D_p = (\sum (W_i / S_i))^{-1} \quad (1)$$

$D_p$  = weighted average particle size,

$S_i$  = average between two adjacent screen sizes,

and

$W_i$  = weight fraction of shale corresponding to size  $S_i$ .

All the oil shale samples are from the Anvil Points mine near Rifle, Colorado, and have been crushed and screened at that site. The size ranges are designated by the size of the screen through which all the shale passes and the size of the screen through which supposedly no particles pass. Unfortunately, the screens are not one hundred per cent

Table 1  
Retorting Test Plan

Retorting Series No.	Tracer Series Number	Particle Sizes (m)			Core Diameter (m)
		Annulus	Core	Top	
S71	1	.152 x .013	.102 x .051	.152 x .013	.457
S72	2	.152 x .013	.102 x .025	.152 x .013	.305
S73	3	.152 x .013	.102 x .076	.152 x .013	.305
S74	4	.152 x .013	.102 x .076	.152 x .013	.610
S75	4B	.152 x .013	.102 x .076	.102 x .051*	.610
S76	2B	.152 x .013	.102 x .025	.102 x .051*	.305

\* Different shale batch than used in core

Table 2  
Screen Analyses And Weighed Average Particle Sizes

Screen Size (m)	Percent Retained				
	0.152 x 0.013	0.102 x 0.025	0.102 x 0.051*	0.102 x 0.051**	0.102 x 0.076
0.1524	--	--	--		
0.1270	15.47	--	--		
0.1016	2.87	--	--		
0.0762	19.30	8.21	3.14	7.89	63.28
0.0635	not used	not used	not used	50.12	not used
0.0539	23.29	4.75	37.68	26.22	28.42
0.0381	14.87	36.50	52.66	5.34	4.77
0.0267	13.88	37.37	3.86	1.62	0.08
0.0188	6.38	11.23	0.97	0.70	0.41
0.0133	2.07	1.08	0	0.46	0.41
0.0094	0.16	0.22	0	0.46	0
0.0067	0.32	0.22	0	0.23	0.41
0.0047	0	0.22	0	0.70	0
0.0033	0	0	0	2.32	0
0.0024	0	0	0	1.86	0
PAN	0.96	0.22	1.45	1.86	1.24
Weighted Average Diameter	0.0519	0.0363	0.0521	0.0344	0.0741

\* Shale used in core

\*\* Shale used in top section of the retort for S75 and S76

efficient and each shale batch includes particles smaller than the smallest screen size. Two batches of  $0.10 \times 0.05$  meter ( $4 \times 2$  inch) shale are needed because there is a change in loading procedure between runs S74 and S75 requiring more of this size range shale. Since the shale is from different crushing and screening runs the properties are different. Runs S75 and S76 are loaded with a top layer of the  $0.10 \times 0.05$  meter ( $4 \times 2$  inch) shale instead of the  $0.15 \times 0.01$  meter ( $6 \times \frac{1}{2}$  inch) shale used in the previous runs.

The void fractions in the core and annulus regions of the retort vary considerably from run to run. Table 3 lists the void fractions in the different runs and Table 4 lists the void fractions as a function of particle size range. The void fraction of a region in the retort is defined as the void volume in that region divided by the total volume in that region including the void and rock volumes. The total volume of a region is calculated from the geometry of that region. The void volume is calculated by subtracting the rock volume from the total volume. To calculate the rock volume a sample of the shale is analyzed using the modified Fischer assay method to obtain the Fischer assay oil content of the shale. Using the Fischer assay to specific gravity relationship developed by Smith,<sup>[3]</sup> the average density of the shale can be obtained. The volume of shale in a region is the weight of the shale in a region divided by the density of that shale.

#### Retort Instrumentation

The retort has both thermocouples and tracer probes. The thermocouples are arranged as shown in Figure 2 and are used to track the steam and retorting fronts. More information on the thermal responses

Table 3  
Load Properties for Runs S71 Through S76

	S71	S72	S73	S74	S75	S76
Core Void, percent	40.1	27.8	46.3	52.7	50.8	43.0
Annulus Void, percent	41.0	39.0	39.2	38.1	34.9	42.6
Top Void, percent	41.0	39.0	39.2	38.1	73.2	45.0
Total Void, percent	40.9	38.5	39.5	40.4	44.6	43.3

Table 4  
Particle Size Ranges and Void Fractions

Particle Size Range (m)	D <sub>p</sub> (m)	S71	S72	S73	S74	S75	S76
0.102 x 0.076	0.0741	-	-	0.463	0.527	0.508	-
0.102 x 0.051	0.0521	0.401					
0.102 x 0.051*	0.0344	-	-	-	-	0.732	0.450
0.102 x 0.025	0.0363	-	0.278	-	-	-	0.430
0.152 x 0.013	0.0519	0.410	0.390	0.395	0.381	0.349	0.426

\* Shale used only in top section of retort for S75 and S76.

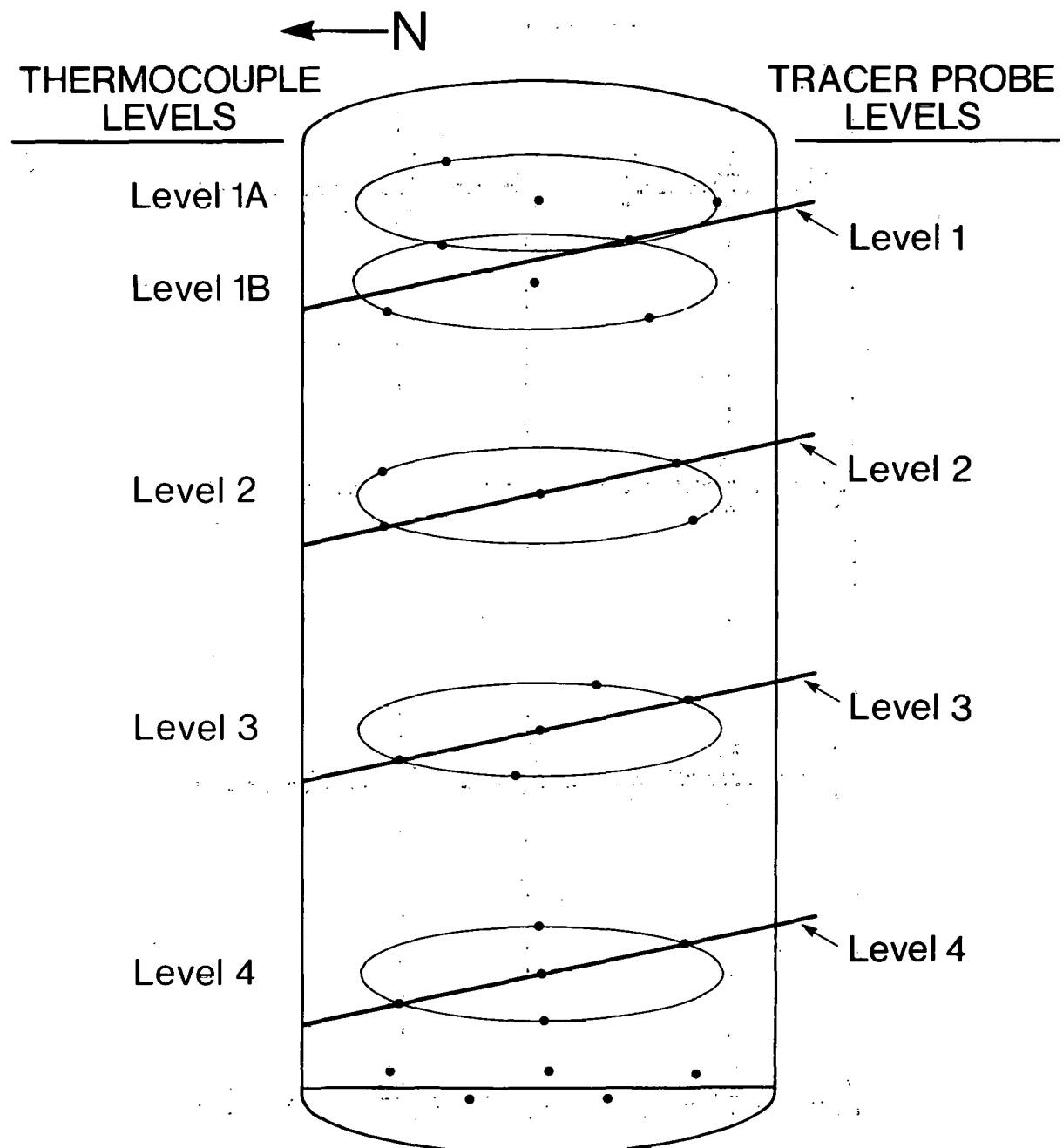


**Figure 2. Thermocouple and Tracer Probe Positions**

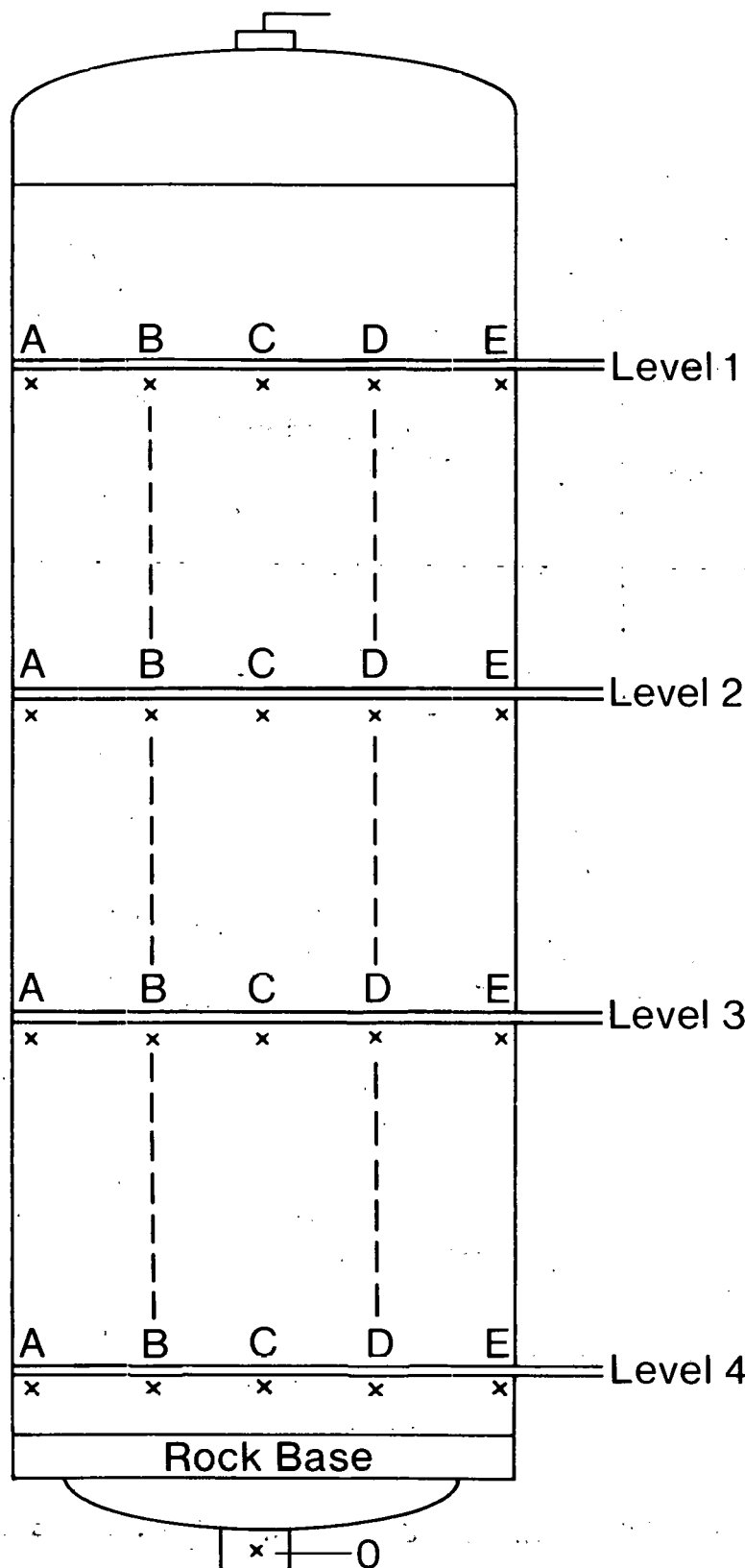


**Figure 3. Tracer Port Locations**

can be found elsewhere.<sup>[2]</sup> As shown in Figure 3, tracer probes are located at 0.91 meter (36 inch) intervals starting 0.58 meters (23 inches) from the top flange. Each probe allows access to five tracer tap positions including two taps 0.08 meters from the walls, one tap on the center line of the retort, and two taps located on the boundary between the core region and the annulus region. All probes are on the same vertical plane running from the southeast to the northwest. Each of the probes consists of a 0.019 meter (3/4 inch) O.D. tube placed across the retort and extending through a sample port in the retort wall. This tube is slotted at each desired tap location. Inside this tube is a 0.006 meter ( $\frac{1}{4}$  inch) O.D. tube fitted with double O-rings on either side of an opening near the end of the tube. The opening on this sliding tube can be moved to cover any one of the slots in the outside tube. The positive pressure on the retort forces air from the retort through the selected tap and through the sliding tube to the tracer detection system outside the retort. A packing gland at the retort wall prevents gas from escaping from the other slots in the outside tube. The probe levels are numbered one through four, starting at the top of the retort, and the taps at each level are lettered A through E, starting on the northwest side of the retort. In this way each tap can be uniquely described by a two-digit location code. For example tap 2C is on the second probe level and is the middle tap on that level.

#### Tracer Testing

The gas chosen for the tracer testing portion of the experiment is krypton-85. This radioactive gas has been used extensively for tracer testing large oil shale retorts and has been used on smaller scale

retorts by WRI and its predecessors for several years. The use of radioactive gas for a tracer allows a simple, easily expandable detection system to be designed, a schematic of which is shown in Figure 4. Basically the system consists of counting chambers where the disintegrations of the Kr-85 are counted and a data acquisition system that totals and stores the counts.

The tracer injection system has evolved considerably during the test series. The current system is shown in Figure 5. This system uses a timer and a fast precision solenoid valve to release tracer from a constant pressure reservoir. The tracer pulses injected using this system are reproducible and easily characterized. The earlier injection system designs are based on krypton being released from constant volume sample bottles into the retort. These designs depend on accurate pressure measurements for reproducibility. The current system is much more precise. A typical injection has a duration of from .5 to 3 seconds controllable to within about twenty milliseconds.

The tracer test series on each retort test consists of fourteen separate injections in six different taps. Table 5 lists the injection taps and the detection taps for each of the tracer tests. Ten of the tests in the test plan are designed to measure axial velocities at three radial positions and overall inlet to outlet velocities. Four of the tests are designed to indicate flow paths between the core and the annulus of the rubble bed.

The tracer tests on the 10-ton retort have been run at a superficial gas velocity (SGV) of 0.00635 meters per second (m/s). The SGV is defined as the volumetric flow rate at standard conditions divided by the total cross-sectional area of the rubble bed. This value for the

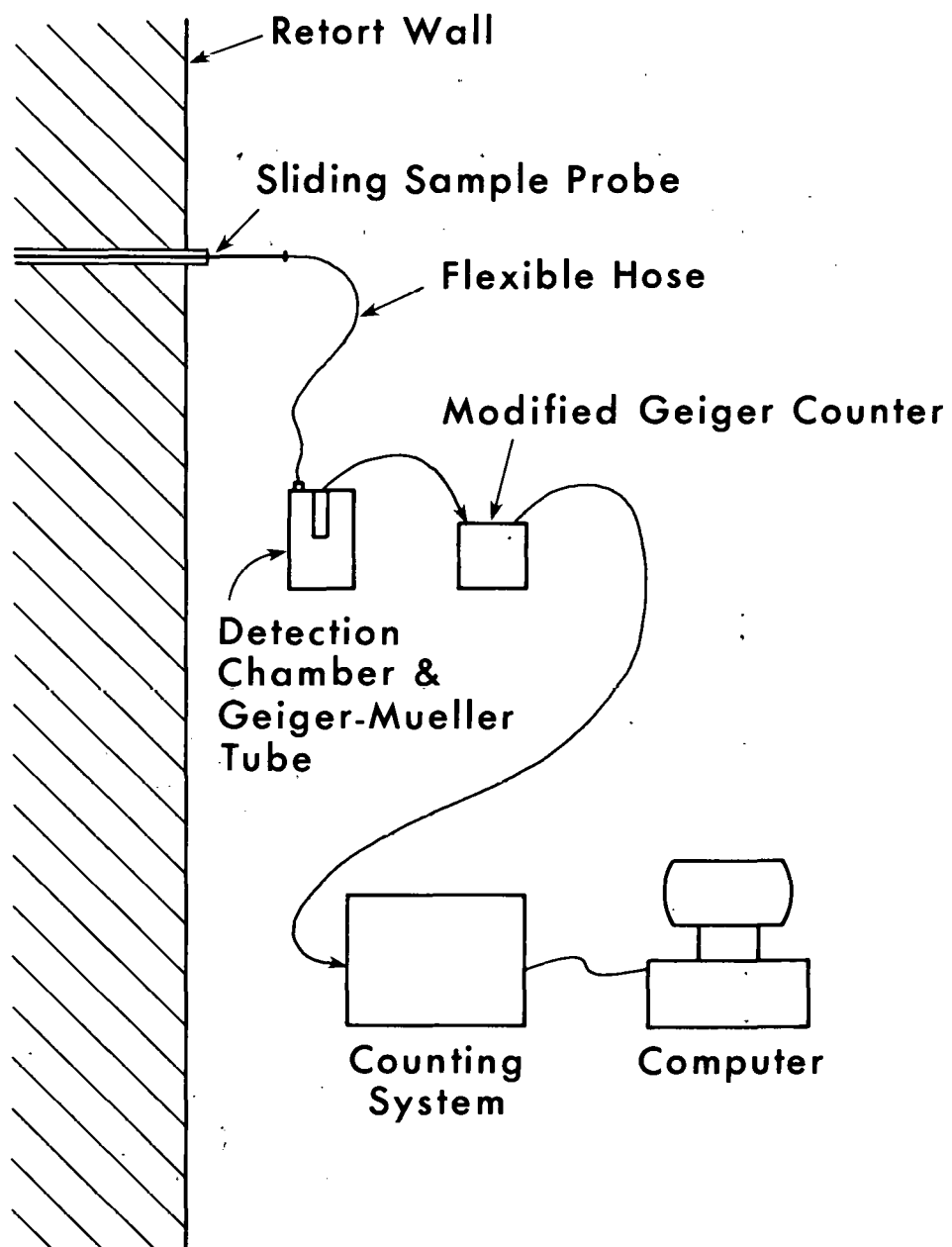


Figure 4. Tracer Detection System

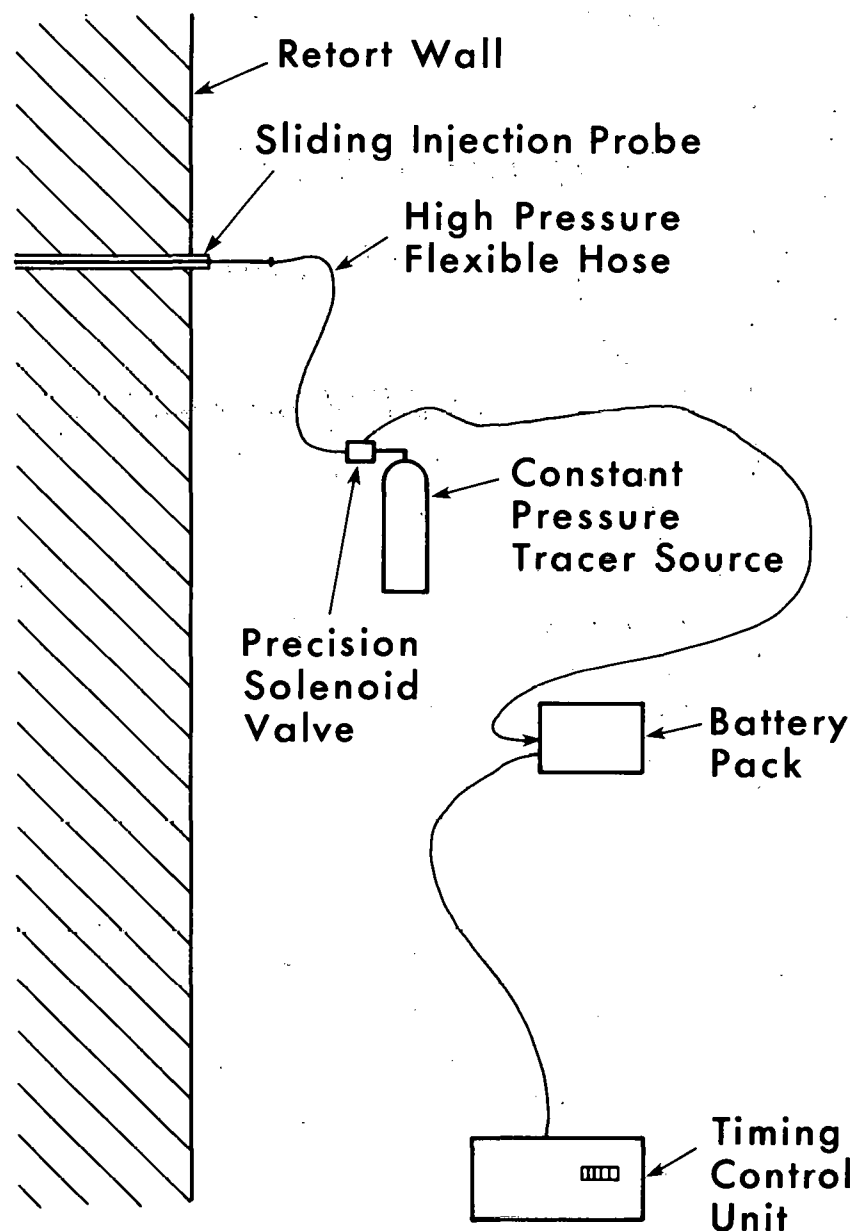


Figure 5. Tracer Injection System

SGV is somewhat higher than is used in MIS retorts (usually less than 0.005 m/s), but the fluid velocity is nearly the same due to the difference in void fraction. During both the tracer tests and the retorting tests the retort is run at a positive gauge pressure of 20.685 kPa. This positive pressure is the driving force for flow in the tracer sampling lines.

Table 5  
Tracer Test Plan for 10-Ton Retort

Test Number	Injection Tap	Detection Taps
1	Inlet	1A,2A,3A,4A,Outlet
2	1A	2A,3A,4A,Outlet
3	Inlet	1B,2B,3B,4B,Outlet
4	1B	2B,3B,4B,Outlet
5	Inlet	1C,2C,3C,4C,Outlet
6	1C	2C,3C,4C,Outlet
7	Inlet	1D,2D,3D,4D,Outlet
8	1D	2D,3D,4D,Outlet
9	Inlet	1E,2E,3E,4E,Outlet
10	1E	2E,3E,4E,Outlet
11	1C	2A,3A,4A,Outlet
12	1C	2E,3E,4E,Outlet
13	1A	2C,3C,4C,Outlet
14	1E	2C,3C,4C,Outlet

## MODEL

A computer program for modeling flow in porous media has been developed by Bryan Travis of Los Alamos National Laboratories (LANL). This model uses a finite difference scheme to solve equations describing mass conservation, tracer concentration and conservation of momentum. [4] The primary model input parameters that determine flow are particle size, void fraction, permeability and either the top and bottom pressures or the velocity at the bottom of the retort. Tracer injection is specified by the time, location and concentration of the injected mixture. The primary outputs of the model are velocity and either pressure or tracer concentration.

The model uses the Ergun equation.

$$U \left(1 + \frac{1.75 \rho D_p}{150(1-\varepsilon)\mu} |U| \right) = -(K/\mu)(\nabla P - \rho g) \quad (2)$$

where  $U$ ,  $K$ ,  $\mu$ ,  $\nabla P$ ,  $\rho$  and  $g$  are the SGV, permeability, fluid viscosity, pressure gradient, fluid density and gravitational acceleration respectively. The permeability input parameter ( $K$ ) is related to the porosity ( $\varepsilon$ ) and effective particle diameter ( $D_p$ ) by the relationship

$$K = \frac{\varepsilon^3 D_p^2}{150(1-\varepsilon)^2} \quad (3)$$

which is consistent with Ergun's equation. [5] Minster and Fausett [6] discuss the origin, limitations and application of equation (2) and the use of a shape factor and other modifications to the Ergun equation. A shape factor is added to the Ergun equation by substituting  $\phi_s D_p$  for  $D_p$  in equations (2) and (3). Based on data from 22 experiments on raw

crushed oil shale Minster and Fausett have determined that  $\phi_s = 0.47$  is an appropriate value. This value is used with the Travis model for the present work.

The retort is represented by the model as a two-dimensional grid of cells in the plane of the probes. Pressure and concentration are calculated for each cell and the velocity is calculated perpendicular to each cell boundary. For the present work, a square cell cross section  $7.62 \times 10^{-2} \text{ m}$  on a side is used. This is a reasonable size considering the particle size distribution and the retort geometry. If the cell size is made too large the distinction between the core and the annulus is lost. If the cell size is made too small the apparent improvement in spatial resolution is misleading because the particle size must be small relative to the cell size if the permeability and porosity of the crushed shale are to apply to a single cell.

The model prints the tables of tracer concentration data on a timetable based on the tracer test data. To observe peaks having short residence times (less than 110 seconds) more frequent printing is chosen to achieve approximately the same peak resolution as for peaks having long residence times. For the first 110 seconds of simulated problem time a table of tracer concentration versus cell location is printed every 5 seconds. For longer problem time a resolution of 15 seconds is used.

## DISCUSSION

### Method of Analysis

Analysis of tracer response data is complicated by the presence of noise in the response curves caused by random disintegrations of the radioactive tracer. This noise causes curve analyses based on the

moments of the response curves to be in error. For example, the mean residence time of a tracer response is defined as

$$\tau_c = \frac{\int_0^\infty tC(t)dt}{\int_0^\infty C(t)dt} \approx \frac{\sum tC(t)}{\sum C(t)} = \tau_e \quad (4)$$

where

$t$  = time

and

$C(t)$  = concentration at time  $t$ .

Equation (4), which is also called the first moment of the curve, shows that the large values for time,  $t$ , near the end of the response curve cause any perturbation in the concentration,  $C(t)$ , to be exaggerated in numerical estimation of  $\tau_c$ . The numerical estimate of  $\tau_c$  will be called  $\tau_e$ . The usual result is an overestimate of the mean residence time. The same phenomenon is seen with the second central moment, or variance, of the curve. Because of these effects, a one-dimensional, three-parameter dispersion model is being used to determine the tracer response curve characteristics.

The one dimensional dispersion model<sup>[7]</sup> is written as

$$C(t) = \frac{A\tau^{\frac{1}{2}}}{(2\pi\tau(\frac{2D}{vL})^{\frac{1}{2}})} \exp \left[ -\frac{(t-\tau)^2}{2\tau(\frac{2D}{vL})} \right] \quad (5)$$

where  $C(t)$ , and  $t$  are as defined above and

$A$  = response curve area,

$\tau$  = space time,  $L/v$

and

$D/vL$  = is the vessel dispersion number

where

$D$  = the axial dispersion coefficient

$v$  = mean fluid velocity magnitude

and

$L$  = distance between injection and detection ports.

The values of  $A$ ,  $\tau$  and  $(\frac{2D}{vL})$  are allowed to vary to fit the experimental response curves. A non-linear regression program is used to fit equation (5) to the data.<sup>[8]</sup> This form of the dispersion model is appropriate for use when the tracer is injected instantaneously into the rubble and the detection tap is in the rubble. The space time,  $\tau$ , is related to the mean residence time  $\tau_c$  by the equation

$$\tau = \tau_c / (1 + (\frac{2D}{vL})) \quad (6)$$

which is discussed in reference [7].

The parameter  $2D/vL$ , or (2/Peclet number), is of interest because for packed beds where the Reynold's number,  $Re$ , is less than five a ratio of particle size to void fraction can be calculated. This parameter can be rewritten as

$$2/Pe = 2D/vL = (2D/vD_p)(D_p/L) \quad (7)$$

or

$$2D/vL = (2D\varepsilon/vD_p)(1/L)(D_p/\varepsilon) \quad (8)$$

where

$D_p$  = particle diameter,

and

$\varepsilon$  = void fraction,

and all other variables are as previously defined. For Reynolds numbers defined as

$$Re = D_p v_p / \mu \quad (9)$$

where

$\rho$  = gas density,

between five and 100 the value of the first term on the right side of equation (8),  $2D\varepsilon/v D_p$ , has been found to be approximately one. [7,9]

Below a Reynolds number of five the value of  $2D\varepsilon/v D_p$  may rise depending on the molecular diffusivity of the gas. The result is that for restricted values of  $Re$ ,  $D_p/\varepsilon L$  is proportional to  $2D/vL$  and a particle size to void fraction ratio can be obtained. During these tests the Reynolds number is about 10.

For each of five retorting tests (S71 - S75) two tables are presented. The first table displays estimated mean residence times ( $\tau_e$ ), peak arrival times ( $t_{pk}$ ), and estimated space times ( $\tau$ ). The values of  $\tau_e$  are obtained by numerical evaluation of equation (4). The space time ( $\tau$ ) is one of the parameters determined by fitting equation (5) to the tracer data. The peak arrival time ( $t_{pk}$ ) is the time corresponding to maximum concentration of the tracer response curve. The second table provides estimates of  $D_p/\varepsilon$ ,  $D_p$  and  $\varepsilon$  using equations (7) and (8). For test S76 only the first table is provided since the dispersion model can

not be fit to the data. The reasons for this are discussed in the section about test S76. In the discussion that follows the space times,  $\tau$ 's, between levels are compared qualitatively for each test. These space times are related to apparent fluid velocity in the rubble by  $v = \frac{L}{\tau}$ .

### Test S71

Data from the response curves for test S71 are shown in Table 6. An interesting feature of the response times is that there is a low residence time channel from 2C through 4C, yet, the residence time from 1C to 2C is relatively high. There are also high residence time regions between levels three and four except at the core. Gas flow from 1C to 4C shows the shortest residence time channel in the retort. These residence times indicate that there is a low permeability region at the top of the central channel and that much of the flow in that channel consists of gas entering the channel from the sides below the first probe level. The decreasing differences in residence times in the channel are probably caused by more flow entering the channel farther down in the retort. This idea is supported by the fact that the residence times on each side of the channel between levels 3 and 4 indicate decreasing velocities.

Values for  $D_p/\varepsilon$  have been calculated for tracer tests between level one and level two to show the accuracy of the dispersion model for short distances. The values of  $D_p/\varepsilon$  for level one-to-level four tests show the accuracy for longer distances. The results are listed in Table 7 along with values of both  $D_p$  and  $\varepsilon$  when measured values of the other parameter are assumed. The parameter,  $2D\varepsilon/vD_p$ , is assumed to be equal

Table 6  
S71 Response Curve Data

Inj	Det	$\tau_e$	$t_{pk}$	$\tau$
1A	2A	70	51	58
	3A	148	122	126
	4A	229	194	206
1B	2B	115	90	99
	3B	205	170	180
	4B	306	270	282
1C	2C	118	102	110
	3C	173	153	162
	4C	210	194	198
1D	2D	211	153	178
	3D	256	224	230
	4D	343	326	317
1E	2E	113	81	90
	3E	210	173	179
	4E	314	255	279

Table 7  
S71 Calculated  $D_p$  and  $\varepsilon$

Inj	Det	$2D/vL$	$D_p/\varepsilon$	$D_p(\text{m})^*$	$\varepsilon^{**}$
1A	2A	.159	.145	.0596	.359
	4A	.054	.148	.0607	.352
1B	2B	.0880	.0804	.033	.648
	4B	.0757	.208	.0851	.251
1C	2C	.0798	.0729	.0299	.715
	4C	.0435	.119	.0489	.438
1D	2D	.145	.133	.0543	.392
	4D	.0727	.199	.0818	.262
1E	2E	.160	.146	.060	.357
	4E	.0570	.156	.0641	.334

\*  $\varepsilon = .41$   
\*\*  $D_p = .0521$

to one for this comparison.<sup>[7,9]</sup> If the particle sizes are assumed to be accurate, the values for  $\varepsilon$  in the level one-to-level two tests are of the right order of magnitude but the  $\varepsilon$  near the center of the retort is too high to be realistic. If the void fractions are assumed to be accurate, the values for  $D_p$  seem realistic except at the center of the retort. Probably the loading of a shale with a large proportion of fine material intermixed over a shale with fewer fines causes infiltration of fines into the larger shale, resulting in a locally lower average particle size and a locally lower void fraction. This effect has been documented,<sup>[10]</sup> and can be seen even if the average particle sizes of the two shales are nearly the same because the two shales could have vastly different ranges of particle sizes. The shale size distribution data in Table 2 supports this idea. If this is truly what is happening, then the low particle size calculated at the center of the retort is most likely an overestimate since the void fraction is probably also too large.

The values of  $D_p/\varepsilon$  for level one to level four are higher than reasonable, resulting in high estimates for  $D_p$  and low estimates for  $\varepsilon$ . Generally, however, the void fraction in the center of the retort appears to be higher than in the annulus. This is not seen in the experimental void fraction data in Table 3.

### Test S72

Data from the response curves for test S72 are shown in Table 8. Again the residence time from 1C to 2C is almost as high as the difference between the times at 2C and 4C. Also, the differences in residence times decrease as the gas moves farther down the channel. As in the

Table 8  
S72 Response Curve Data

Inj	Det	$\tau_e$	$t_{pk}$	$\tau$
1A	2A	80	61	61
	3A	146	112	118
	4A	212	173	179
1B	2B	135	110	118
	3B	256	220	232
	4B	285	240	261
1C	2C	106	92	93
	3C	173	143	153
	4C	204	183	190
1D	2D	223	190	178
	3D	262	220	230
	4D	313	290	317
1E	2E	77	60	62
	3E	184	150	156
	4E	313	270	277

Table 9  
S72 Calculated  $D_p$  and  $\epsilon$

Inj	Det	$2D/vL$	$D_p/\epsilon$	$D_p(m)$	$\epsilon$
1A	2A	.112	.102	$\epsilon = .39$ .0399	$D_p = .0521$ .511
	4A	.0653	.179	.0699	.291
1B	2B	.0984	.090	.0351	.579
	4B	.0728	.200	.0779	.261
1C	2C	.0855	.0782	$\epsilon = .278$ .0217	$D_p = .0366$ .468
	4C	.0501	.137	.0382	.267
1D	2D	.145	.133	$\epsilon = .39$ .0517	$D_p = .0521$ .392
	4D	.0727	.199	.0778	.262
1E	2E	.129	.118	.0460	.442
	4E	.0629	.173	.0673	.301

case of S71 there seems to be a low permeability region between 1C and 2C that slows the gas flow to 2C. From 2C to 4C, however, the difference in residence times is low. The lowest residence time flow path is on the A side of the retort.

The values for  $D_p/\varepsilon$  for tracer tests between level one and levels two and four are listed in Table 9. Also listed are values for  $D_p$  and  $\varepsilon$  for measured retort properties. If the void fractions in the retort calculated from the loading weights are correct, then the particle sizes are low. The particle size at the center is lower than in the annulus. This is also seen in Table 2 for the screening data.

The values of  $D_p/\varepsilon$  for the level one-to-level four tests are again high resulting in high estimates for  $D_p$  and low estimates for  $\varepsilon$  except at the center. The general trend is that the particle size in the center of the retort is smaller than in the annulus.

### Test S73

Data from the response curves for test S73 are shown in Table 10. The residence time between 1C and 2C is low. The differences in residence times below 2C indicate an increase in velocity farther down the retort, caused by movement of gas into the channel. Residence times on the D side of the channel are high all the way down the retort. The lowest level one-to-level four residence time is on the A side of the retort.

Values for  $D_p/\varepsilon$  are listed in Table 11 as are the values of  $D_p$  and  $\varepsilon$ . In this test the value of  $D_p$  at the center of the retort is higher than the  $D_p$  on each side of the core. The void fraction at the center of the retort is slightly lower than on each side of the core at values of  $D_p$  predicted from the screening data.

Table 10  
S73 Response Curve Data

Inj	Det	$\tau_e$	$t_{pk}$	$\tau$
1A	2A	73	61	63
	3A	136	112	117
	4A	202	163	174
1B	2B	121	102	109
	3B	223	173	191
	4B	283	245	256
1C	2C	182	130	148
	3C	280	230	250
	4C	340	290	309
1D	2D	184	140	159
	3D	278	240	240
	4D	372	320	332
1E	2E	116	90	92
	3E	256	200	208
	4E	349	260	286

Table 11  
S73 Calculated  $D_p$  and  $\varepsilon$

Inj	Det	$2D/vL$	$D_p/\varepsilon$	$D_p(m)$	$\varepsilon$
1A	2A	.137	.125	$\varepsilon = .392$ .0491	$D_p = .0521$ .417
	4A	.0654	.179	.0703	.291
1B	2B	.0832	.0760	.0298	.686
	4B	.0658	.181	.0708	.288
1C	2C	.165	.151	$\varepsilon = .463$ .0699	$D_p = .0729$ .483
	4C	.0793	.218	.1007	.334
1D	2D	.106	.0970	$\varepsilon = .392$ .0380	$D_p = .0521$ .537
	4D	.0693	.190	.0745	.274
1E	2E	.127	.116	.0455	.449
	4E	.102	.280	.110	.186

The level one-to-level four values of  $D_p/\varepsilon$  are again high. Estimates made from  $D_p/\varepsilon$  show that both  $D_p$  and  $\varepsilon$  are higher in the core than to each side of the core. Overall the values of  $D_p$  are higher than expected and the values of  $\varepsilon$  are lower than expected from the screen analysis and load data.

#### Test S74

Data from the response curves for test S74 are shown in Table 12. The highest residence times in the retort are from 1C to all other taps in the core. Interestingly, the residence time from 1C to 2C is nearly the same as that from 1C to 3C. The implication of this phenomenon is that most of the gas in the core is entering from the sides at or below 2C. The lowest residence times in the retort are along the walls.

The values for  $D_p/\varepsilon$  for this test are listed in Table 13 along with values for  $D_p$  and  $\varepsilon$ . For level one-to-level two tests, the values of  $D_p$ , when  $\varepsilon$  is calculated from load data, are low except at the center. The value of  $D_p$  here is higher than estimated from the screen analysis data. If this particle size is assumed to be as screened, the value for  $\varepsilon$  is lower than predicted from loading data but is more reasonable. This value for  $\varepsilon$  (in the core) is lower than the void fractions calculated for each side of the core.

The level one-to-level four values of  $D_p/\varepsilon$  show high values for  $D_p$  and low values for  $\varepsilon$ . The core has a higher particle size and a lower void fraction than does the annulus.

Table 12  
S74 Response Curve Data

Inj	Det	$\tau_e$	$t_{pk}$	$\tau$
1A	2A	80	70	71
	3A	140	120	127
	4A	190	170	177
1B	2B	112	90	98
	3B	188	180	177
	4B	241	229	230
1C	2C	708	520	601
	3C	744	520	638
	4C	807	622	723
1D	2D	113	92	97
	3D	220	204	195
	4D	332	275	308
1E	2E	71	50	58
	3E	130	100	--
	4E	205	160	174

Table 13  
S74 Calculated  $D_p$  and  $\varepsilon$

Inj	Det	$2D/vL$	$D_p/\varepsilon$	$D_p(m)$	$\varepsilon$	
1A	2A	.0828	.0757	$\varepsilon = .381$ .0289	$D_p = .0521$ .688	
	4A	.0645	.177	.0674		.294
1B	2B	.0912	.0834	.0318		.625
	4B	.0564	.155	.0590		.336
1C	2C	.200	.183	$\varepsilon = .527$ .0964	$D_p = .0729$ .398	
	4C	.161	.442	.233		.165
1D	2D	.103	.0942	$\varepsilon = .381$ .0359	$D_p = .0521$ .553	
	4D	.0737	.202	.077		.258
1E	2E	.143	.131	.0498		.398
	4E	.0881	.242	.0921		.215

### Test S75

Test S75 is the first test in this test series in which the particle size above the core has been changed. This has been done in an effort to prevent the formation of a low permeability region at the top of the core. Data from the response curves for test S75 are shown in Table 14. The highest residence times are on the CDE side of the retort. The differences in residence times farther down in the retort at C, D, and E decrease, indicating gas flow into this region. The residence times at A and B are nearly equal and are much lower than the times on the other side of the retort.

The values of  $D_p/\varepsilon$ ,  $D_p$ , and  $\varepsilon$  are listed in Table 15. These numbers show that if the void fractions calculated from the loading data are correct, then the particle sizes on the AB side of the retort are low but equal, the particle size at C is higher than reasonable, the particle size at D is in agreement, and at E is low. If the particle size calculated from the screening data is assumed correct, then  $\varepsilon$  is reasonable on the AB side of the retort, low at C and D, and high at E.

The values for  $D_p/\varepsilon$  for the level one-to-level four tests are high. The calculated values for  $D_p$  and  $\varepsilon$  show high  $\varepsilon$  and  $D_p$  in the core.

### Test S76

Test S76 is a retort test using the same run conditions as in test S72 with the exception that S76 has a top layer of  $0.10 \times 0.05$  meter shale instead of the  $0.15 \times 0.01$  meter shale used in S72. The response curve data for test S76 are listed in Table 16. Because of very long tails on the peaks, the values for  $\tau_e$  are high and curve fitting with the one-dimensional dispersion model is impossible. The numbers for  $\tau$

Table 14  
S75 Response Curve Data

Inj	Det	$\tau_e$	$t_{pk}$	$\tau$
1A	2A	106	60	92
	3A	209	170	188
	4A	291	267	278
1B	2B	120	89	99
	3B	232	184	202
	4B	283	234	260
1C	2C	248	246	201
	3C	313	257	275
	4C	389	336	361
1D	2D	349	258	304
	3D	413	375	372
	4D	448	413	411
1E	2E	264	199	216
	3E	377	305	325
	4E	438	361	393

Table 15  
S75 Calculated  $D_p$  and  $\varepsilon$

Inj	Det	$2D/vL$	$D_p/\varepsilon$	$D_p(m)$	$\varepsilon$	
1A	2A	.137	.125	$\varepsilon = .349$	$D_p = .0521$	
	4A	.0612	.168	.0437	.417	.310
1B	2B	.133	.122	.0424		.427
	4B	.0661	.181	.0633		.288
1C	2C	.228	.208	$\varepsilon = .508$	$D_p = .0729$	
	4C	.0768	.211	.106	.351	.346
1D	2D	.162	.148	$\varepsilon = .349$	$D_p = .0521$	
	4D	.0847	.232	.0517	.352	.225
1E	2E	.102	.093	.081		.559
	4E	.0972	.267	.0325		.195
				.0931		

Table 16  
S76 Response Curve Data

Inj	Det	$t_{pk}$	$\tau^*$
1A	2A	59	64
	3A	119	129
	4A	182	197
1B	2B	65	70
	3B	120	130
	4B	196	212
1C	2C	59	64
	3C	113	122
	4C	161	174
1D	2D	72	78
	3D	133	144
	4D	174	188
1E	2E	45	49
	3E	89	96
	4E	181	199

\* Estimate for  $\tau$  based on equation (10).

in Table 15 are derived from a correlation between  $t_{pk}$  and  $\tau$  developed from tests S71 through S75. This correlation has the form

$$\tau = 1.0802 t_{pk} \quad (10)$$

for which the coefficient of determination,  $r^2$ , is .919, based on all the  $t_{pk}$  and  $\tau$  data from the earlier tests. This correlation is used to calculate  $\tau$  for S76.

The residence time in the core from 1C to 4C is lower than in any other level one-to-level four path. This is dramatically different from

test S72 in which the flow in the channel is blocked near the top, resulting in long response times for the taps lower in the channel.

#### Comparison of Tracer and Flow Model Results

For comparison with tracer tests, the 2-D model has been set up with the bed conditions used in tests S72 and S76. The bed conditions are assumed to be those calculated from loading data and from screen analysis. The response times of the tracer peaks are used to calculate apparent fluid velocities for comparison with tracer velocities. All velocities are normalized by dividing by the expected gas velocity in the bed ( $U/\epsilon$ ).

The velocity data for test S72 are shown graphically in Figures 6, 7 and 8. These figures show normalized apparent velocities from level 1 to level 2, level 1 to level 3, and level 1 to level 4, respectively, for both the tracer and model results. The velocities developed from the tracer data do not indicate a mass balance. This is caused by either a higher void fraction in the rubble or a lower flow rate than expected. Qualitatively, the experimental velocity plots show similar characteristics. The velocities in the core and on the core boundaries are low and the velocities on the walls are higher. The flow model shows a low velocity in the core with higher velocities everywhere else. The reasons for the qualitative differences in the model and experimental curves may be in the choices for  $D_p$  and  $\epsilon$  in the model. Table 9 shows that if the particle sizes from the screen analyses are assumed correct, the void fractions between levels 1 and 2 are about the same across the retort except at D. These void fractions along with the assumed particle sizes indicate that flow in the core should not be much

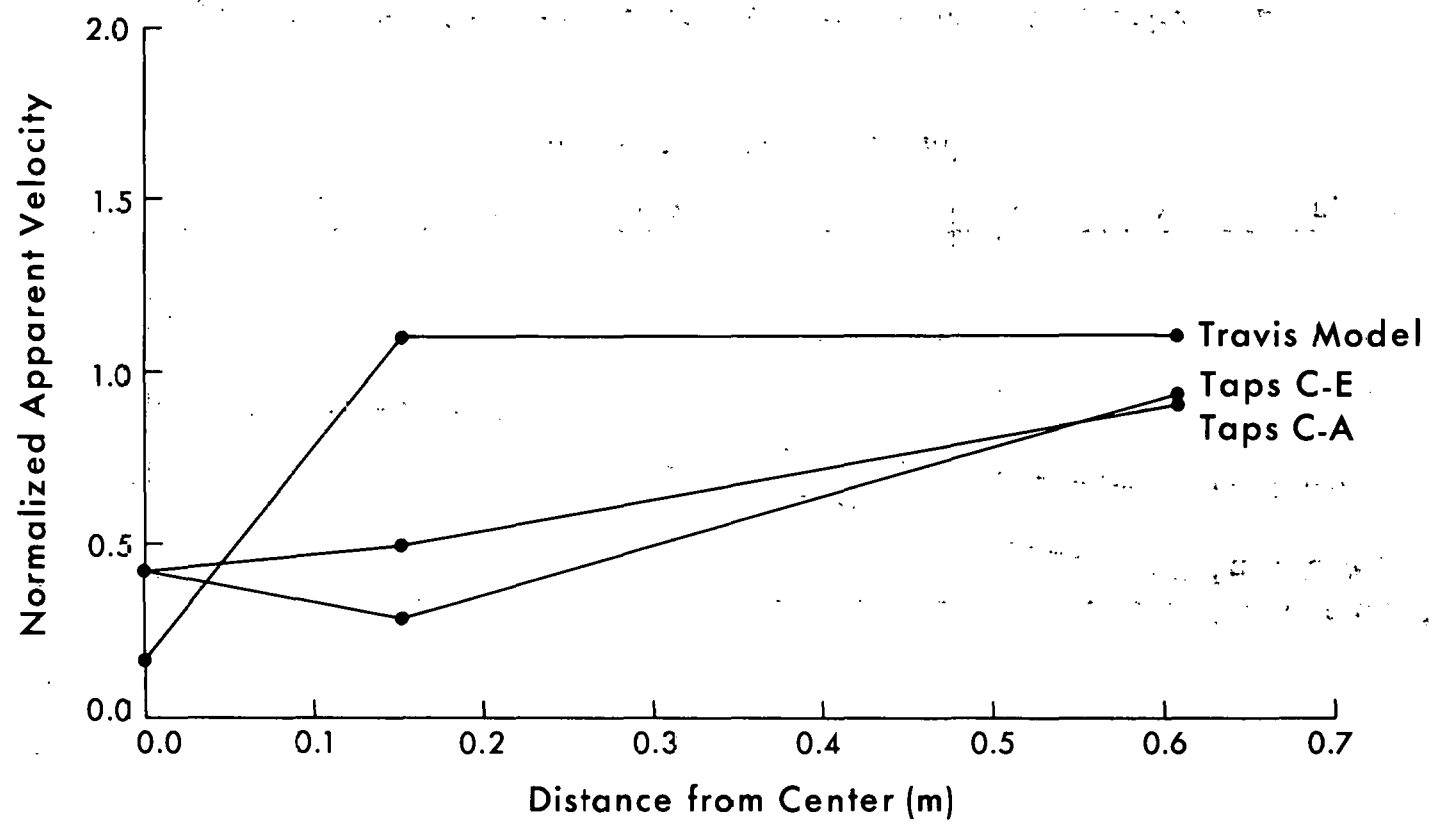


Figure 6. Level 1 to Level 2 Normalized Apparent Velocity, S72

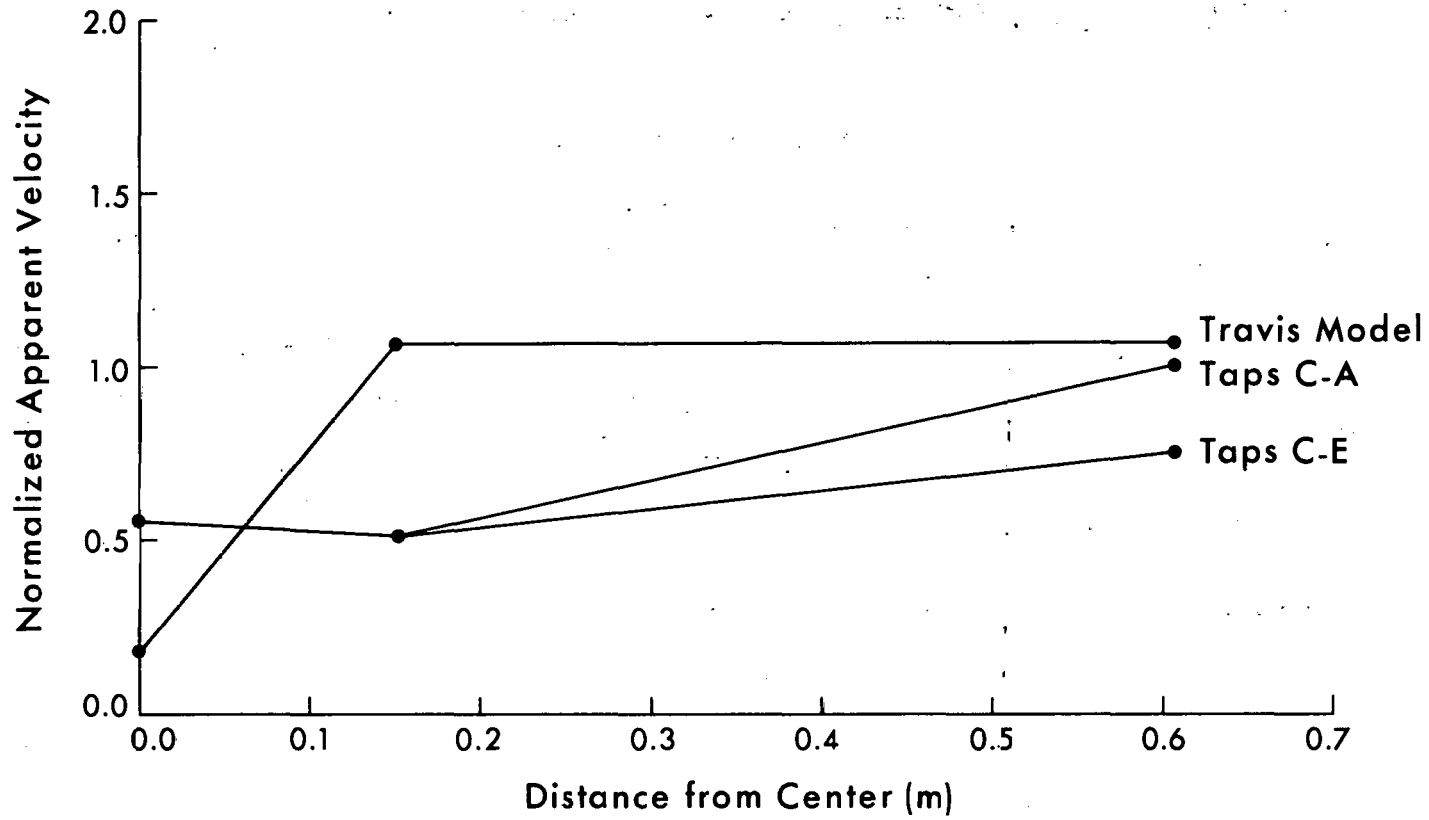


Figure 7. Level 1 to Level 3 Normalized Apparent Velocity, S72

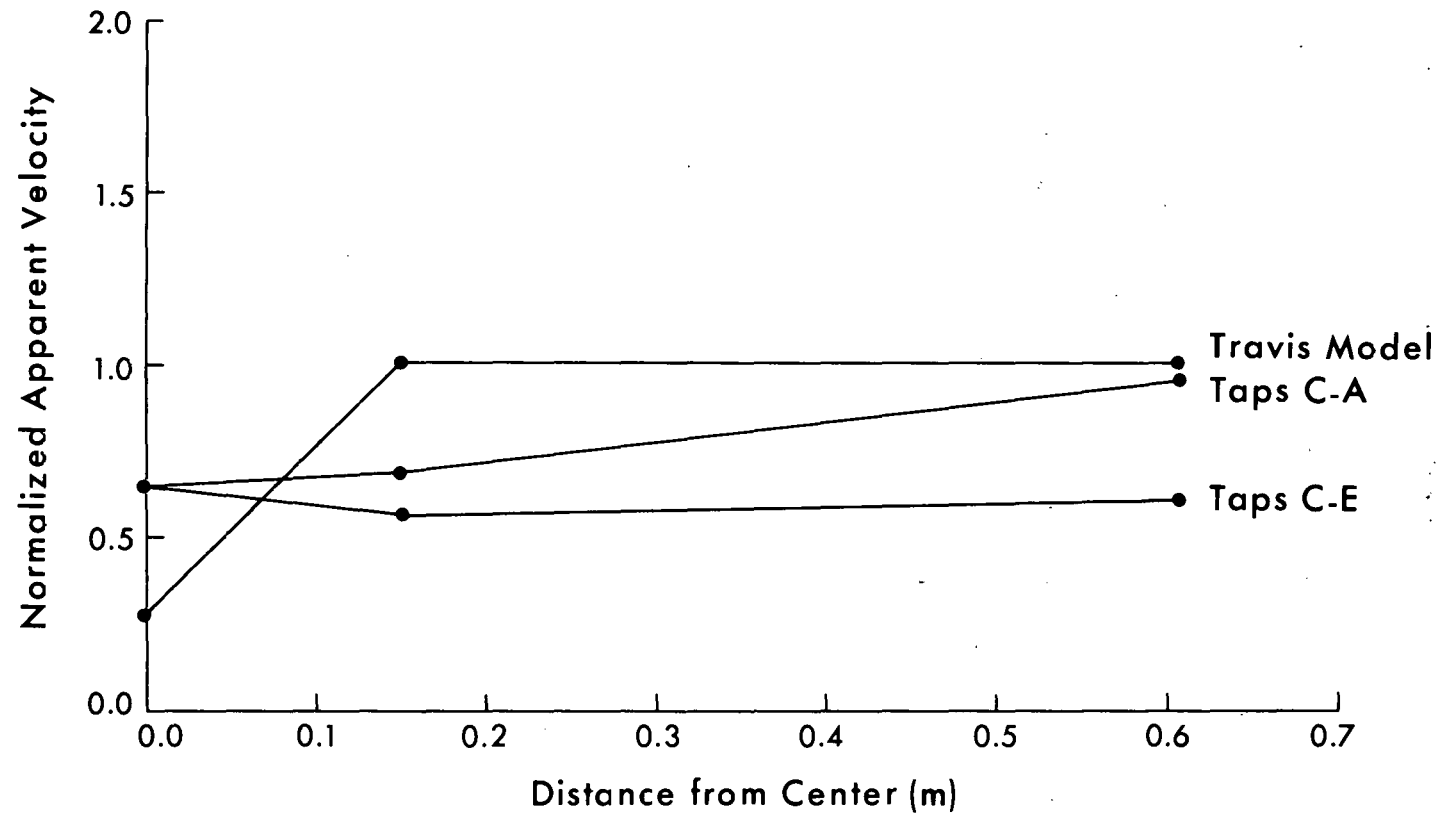


Figure 8. Level 1 to Level 4 Normalized Apparent Velocity, S72

different from the flow at the boundaries of the core. The high experimental velocities at the walls may be the result of a local wall effect. Also, the dispersion model used to generate Table 9 may not be accurate at the walls.

In test S76 much more care has been taken to produce accurate flow rates. This can be seen in Figures 9, 10 and 11 which are the normalized apparent velocity plots for level 1 to levels 2, 3 and 4 respectively for both the flow model and experimental results. In these figures the only major quantitative or qualitative differences between the model and experimental data occur in the core. Since the dispersion model has not been used on S76, there is no way of double checking the particle sizes or the void fraction in the core.

## CONCLUSIONS

The retort loading and operating conditions improved considerably during the test program. This is evidenced by the improvement in the way the gas velocities, as measured by the tracer tests, match the velocities from the Travis model in test S76 as compared to test S72. The change in loading procedure between tests S74 and S75 resulted in more gas flow through the core. A relining of the retort between tests S75 and S76 improved the flow symmetry in the retort as shown by the tracer response times.

The Travis model using  $\varepsilon$  and  $D_p$  calculated from screening and loading data does not always match velocities calculated from tracer tests. This may be caused by inaccuracies in  $\varepsilon$  and  $D_p$ . The dispersion model supports this conclusion on S72 by showing that  $\varepsilon$  is much higher than the load data indicate.

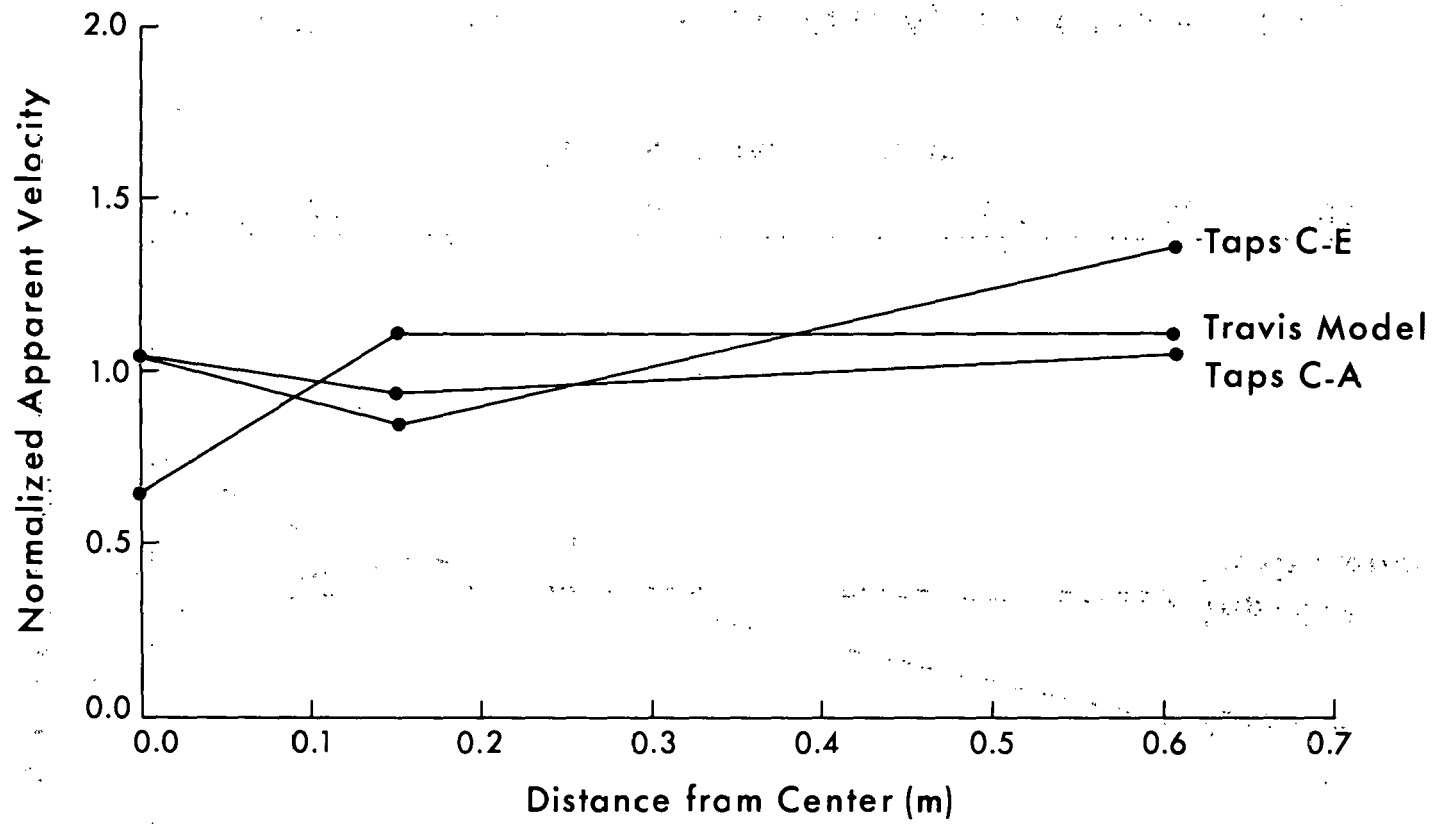


Figure 9. Level 1 to Level 2 Normalized Apparent Velocity, S76

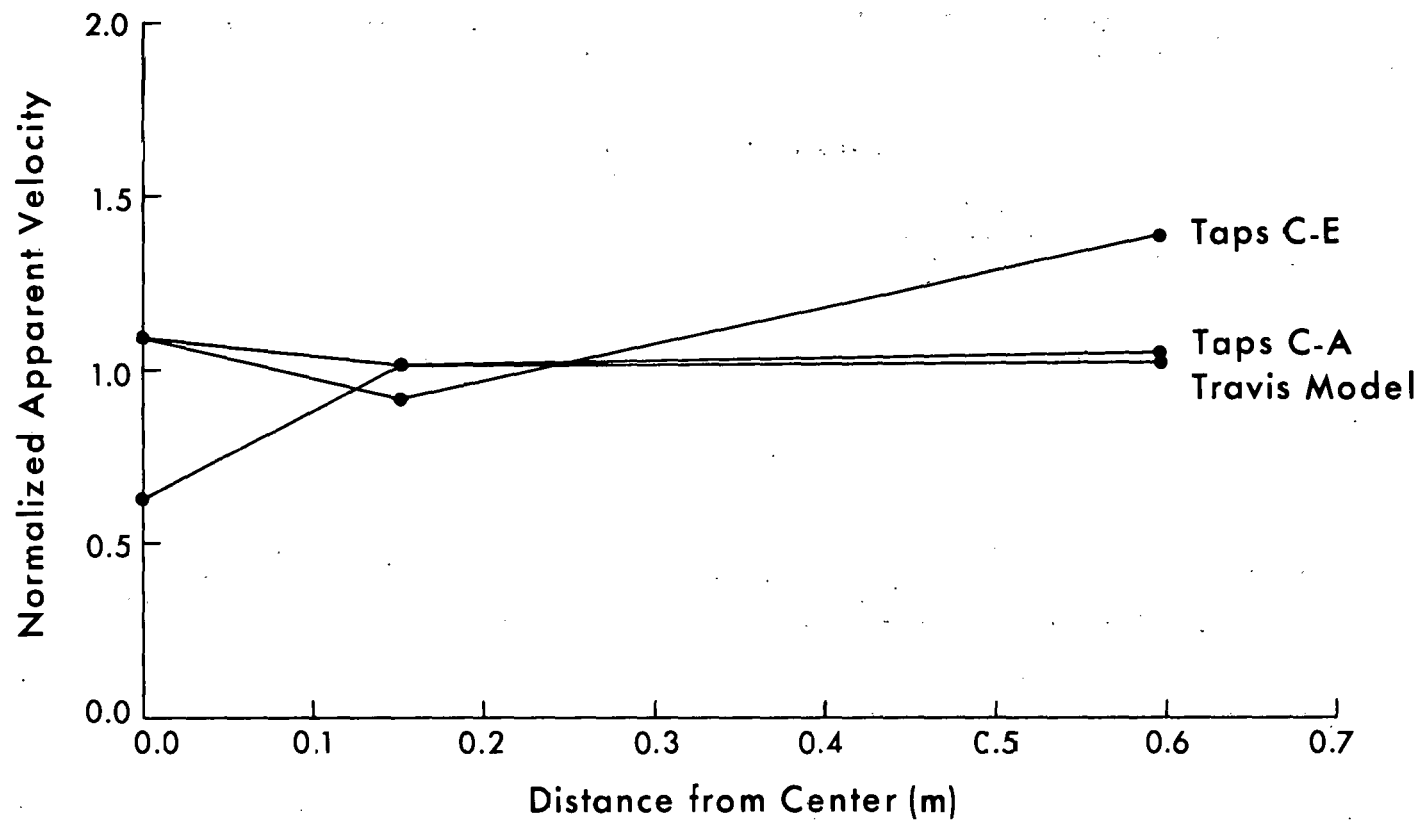


Figure 10. Level 1 to Level 3 Normalized Apparent Velocity, S76

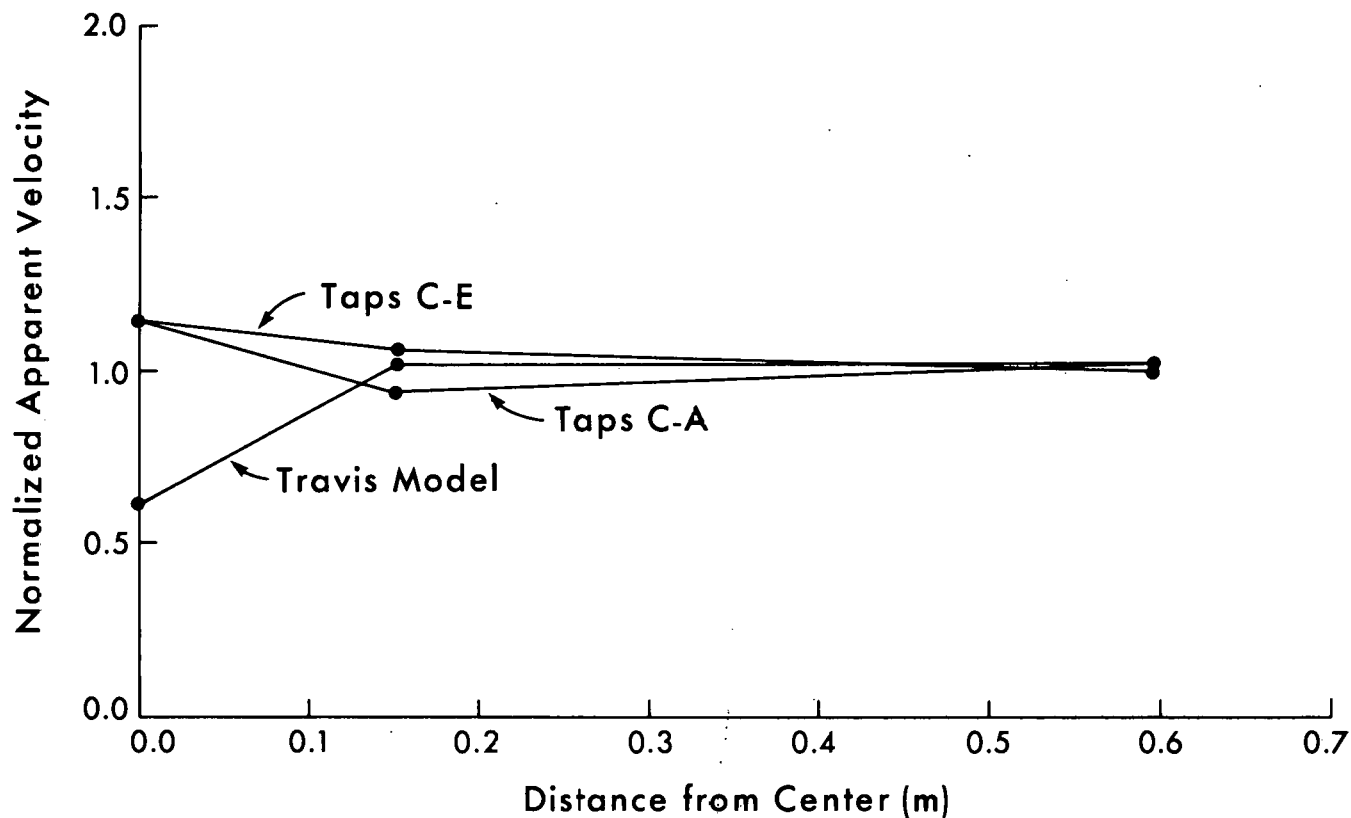


Figure 11. Level 1 to Level 4 Normalized Apparent Velocity, S76

The dispersion model shows signs of being the correct approach to analyzing response curve shapes. The implementation of the dispersion model with boundary conditions corrected for inlet to outlet tracer tests may provide a good overall retort characterization.

#### Recommendations

As an addition to the current 10-ton retort test program a test with a uniform rubble bed should be run. In this test a small average particle size should be used to produce a measurable pressure drop across the retort. This test would provide a known pressure drop which could be compared with the Travis model results. This test would also investigate the behavior of the Travis model at the center of the retort.

Inlet to outlet tracer tests should be compared with inlet to outlet tracer simulations from the Travis model. An inlet to outlet version of the dispersion model should be used to evaluate the rubble bed characteristics for input into the Travis model.

The speed of convergence of the Travis model should be improved so that it can be applied more economically in conjunction with input parameters from the dispersion model.

## References

1. T. F. Turner, D. F. Moore, N. W. Merriam and J. R. Covell, "Investigation of Tracer and Steam Tests on the Western Research Institute 150-Ton Retort", WRI Report, DOE/FE/60177-0001, 1984.
2. N. W. Merriam, J. R. Covell, A. Long and T. F. Turner, "Retorting Oil Shale with Zones of Contrasting Permeability", WRI report in preparation.
3. J. W. Smith, "Specific Gravity--Oil Yield Relationships of Two Colorado Oil Shale Cores", Industrial and Engineering Chemistry, vol. 48, No. 3, 1956, pp. 441-444.
4. B. J. Travis and T. L. Cook, "Numerical Simulation of Fluid Flow in Porous/Fractured Media", 5th AIME Uranium Seminar, 1981, Albuquerque, New Mexico.
5. S. Ergun, "Fluid Flow Through Packed Columns", Chemical Engineering Progress, vol. 48, No. 2, 1952, pp. 89-94.
6. R. A. Minster and D. W. Fausett, "Fluid Flow Through Packed Columns of Crushed Oil Shale", Report of Investigation, U. S. Department of Energy, Laramie Energy Technology Center, Number LETC/RI-80/5, Distribution Category UC-91.
7. O. Levenspiel, Chemical Reaction Engineering (2nd Ed.), 1972, John Wiley and Sons, New York.
8. "Nonlinear Regression for the HP9845", Hewlett-Packard Desktop Computer Divison, P/N 09845-15141, 1979.
9. N. Standish and K. Polthier, "An Interpretation of Tracer Results from an Operating Blast Furnace by a Dispersion Model", Symposium Proceedings, B.F.A. Symposium, Wollongong, Australia, 1975.
10. M. A. Propster, "Gas Flow Phenomena in the Stack Region of the Iron Making Blast Furnace", Doctoral Thesis, State University of New York, 1977.